

A Position Detection Strategy for Sensorless Surface Mounted Permanent Magnet Motors at Low Speed Using Transient Finite-Element Analysis

Z. Wang¹, Shuangxia Niu¹, S. L. Ho¹, W. N. Fu¹ and Jianguo Zhu²

¹Department of Electrical Engineering, The Polytechnic University, Kowloon, Hong Kong

²Faculty of Engineering, University of Technology, Sydney, P.O. Box 123, Broadway NSW 2007, Australia
eeslho@polyu.edu.hk

Abstract — This paper proposes a novel solution for sensorless position detection of conventional surface mounted PM motors. The strategy of the proposed scheme is creatively formulated with a combination of electromagnetic field with transient finite element method (FEM). The proposed solution is an improvement over and above conventional methods in that it is based on rotor position detection at zero speed with high frequency signal injection and back EMF detection. Previous researches tend to consider the induced signal from different winding terminals independently. The proposed methodology however exploits the induced voltage signals from two of the motor winding terminals, using the third terminal as the signal injection point. The strategy also eliminates the process of polarity tests. The relationship between the dependency of induced signals and the rotor position angle is summarized, and a simple motor starting scheme is proposed. Effects arising from the transient characteristics of the injected/induced signals are fully addressed using FEM.

I. INTRODUCTION

Permanent magnet brushless machine is widely used in industry due to its high efficiency and high torque/power density. However, conventional PM brushless machine always requires rotor position information in order to operate satisfactorily. In classical electrical drive systems, the problem of rotor position identification is solved using dedicated mechanical sensors such as encoders, Hall sensors or resolvers. Unfortunately, there are many drawbacks in these sensors, such as limited temperature operation, limited speed, increased cost/size and complexity of system which degrades the overall performance and reliability of the system. In order to reduce cost and system complexity, sensorless control technology is investigated extensively [1-3]. Among the various sensorless techniques, the zero and very low speed position estimation or speed control is one of the most challenging topics for researchers. It is well-known that when the motor is running at mid-speed range, the back EMF induced in the windings can be used for rotor position estimation. When the motor is at standstill, there is however no back EMF induced in the windings, and hence a startup algorithm or an initial rotor position detection method is required in order to start the motor reliably from standstill up to the minimum speed, at which conventional position sensorless control methods based on back EMF information could be implemented.

The most popular sensorless control method for starting and low speed operation is based on injecting a voltage signal into the phase windings and measures the resultant high frequency induced signal. Such a method was originally developed for induction motors, and the

techniques are subsequently extended to PM brushless motors with salient constructions. It is also extended to brushless motor with a surface-mounted PM rotor by utilizing the saliency arising from magnetic saturation. Generally this method is limited to fractional loading conditions with iron saturation. Also, the cross-coupling between d - q axes will heavily influence the accuracy of position estimations. Mathematical analysis of the behavior of the motor in the presence of injected signals is reported in [4-5].

The research reported in this paper creatively applies and improves the above sensorless control strategy onto the BLDC motor to alleviate the starting problem from standstill. It has the following advantages:

1. FEM is utilized to investigate a complete motor model, and hence developing a solid theory-based motor control strategy.
2. The research also improves the signal injection strategy, simplifies the implementation and eliminates the need for polarity detection and hence offering a simple control drive.
3. The biggest advantage is that it utilizes the saliency that surface mounted permanent magnet motor originally possesses, thus eliminating the requirement to modify the rotor structure. This has largely increased the practicability of this strategy because it can be realized in most commonly used PM motors.

II. METHODS

The computation is based on a numerical simulation that uses transient FEM on a common Brushless DC motor model. One of the three phase windings, in this case, Phase A, is used as the signal injection winding. A voltage signal $V = 5\sin(1000 \times 2\pi t)$ is applied to the terminals of Phase A and Neutral wire. The voltage between Phase B and the Neutral wire, V_B , and the one between Phase C and Neutral wire, V_C , are measured.

FEM is used to compute the transient voltages V_B and V_C and then give the variation trend of V_B and V_C as the rotor position changes.

According to two-phase to three-phase transformation, the difference between V_B and V_C for a three phase motor is corresponding to the induced voltage V_b in a two phase motor, in which the variation of V_b is reflecting the rotor's position when a voltage V_a is injected into winding "A".

Since V_B and V_C are always in phase, it makes sense to subtract their amplitudes at different rotor position angles and the variation of their difference V_{BC} against the rotor position is plotted in Fig. 1.

Fig. 1. Variation of V_{BC} as the rotor position changes.

From Fig. 1, one can also see that the amplitude of the voltage difference V_{BC} is relatively small at the position angles from 60° to 120° , and from 240° to 300° . This will give rise to problems for rotor position identification, as the small differences in voltage as observed are insufficient for one to distinguish between the two intervals.

The solution for this problem is to inject the same signal from another phase winding to, for instance, Phase B. Then the difference between the induced voltages V_C and V_A is measured as V_{CA} . V_{CA} has a 120° shift from V_{BC} , and the combination of these two quantities is then providing adequate information for rotor position detection, as summarized below: $0^\circ < \theta < 60^\circ$, the amplitude of V_{BC} is between 60 and 500 mV, and V_B is larger than V_C ; $60^\circ < \theta < 120^\circ$, V_{BC} is quite small at this interval. The amplitude varies between 0 and 60 mV, and there is another interval that shows the same variation trend. In order to distinguish them, another signal is injected into Phase B. Between 60° and 120° , V_{CA} varies between 500 to 700 mV; $120^\circ < \theta < 180^\circ$, the amplitude of V_{BC} is between 60 and 500 mV, and V_B is smaller than V_C ; $180^\circ < \theta < 240^\circ$, the amplitude of V_{BC} is between 500 and 700 mV, and V_B is larger than V_C ; $240^\circ < \theta < 300^\circ$, V_{BC} is also quite small at this interval. The amplitude varies between 0 and 60 mV. When another signal is injected into Phase B, between 240° and 300° , V_{CA} varies between 60 to 500 mV; $300^\circ < \theta < 360^\circ$, the amplitude of V_{BC} is between 500 and 700 mV, and V_B is smaller than V_C .

III. RESULTS

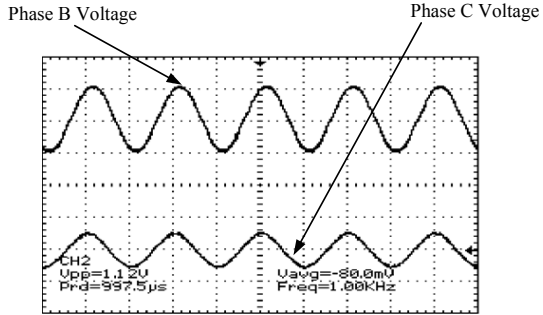
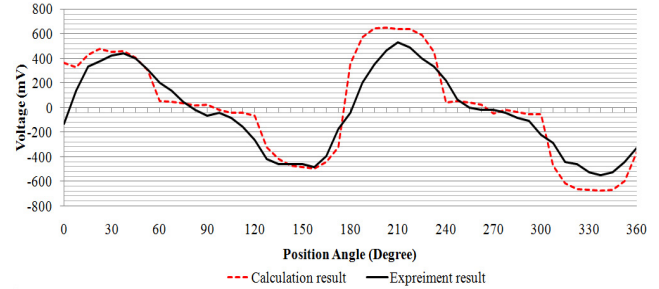
To ensure the accuracy and practicability of the research, a real BLDC motor is considered as the experiment subject and the above model is created based on it.

TABLE I
MOTOR PARAMETERS

Item	Amount
Number of poles	4
Trigger pulse width	120°
Number of slots	6
Winding layers	2
Stator outer diameter	56 mm
Rotor outer diameter	26 mm
Magnet thickness	4 mm
Magnet coercivity	125000 A/m

To verify the simulation results, experiments are carried out. A motor that has the same specifications as in the simulation is used. A function generator is used as the

signal source to inject $V=5\sin(1000\times 2\pi t)$ into Phase A. The waveforms of V_B and V_C are shown in Fig. 2.

Fig. 2. Measured Phase voltage V_B and V_C .Fig. 3. Comparison of V_{BC} variation between the experiment result and simulation results.

Following the same procedures as in the simulation, V_B and V_C are sampled as the rotor position angle θ varies from 0° to 360° at an interval of 7.5° each time. Fig. 3 gives the variation trend of V_{BC} , the difference between V_B and V_C , when a voltage signal is injected into Phase A. As shown in the figure, the voltage difference, i.e. V_{BC} , shows the variation trend that is very close to that of the simulation result. The voltage difference changes from positive to negative or backwards at the same angle as depicted in the simulation. The maximum value in the region from 180° to 240° is also larger than that from 0° to 60° , which agrees with the simulation.

IV. REFERENCES

- [1] W. N. Fu, and S. L. Ho, and Zheng Zhang, "Design of position detection strategy of sensorless permanent magnet motors at standstill using transient finite-element analysis," *IEEE Trans. Magn.*, vol. 45, no. 10, pp.4668-4671, Oct. 2009.
- [2] A. Consoli, S. Musumeci, A. Raciti, and A. Testa, "Sensorless vector and speed control of brushless motor drives," *IEEE Trans. Ind. Electron.*, vol.41, no.1, pp.91-96, Feb. 1994
- [3] P. Pillay and Krihsnan R. Modeling, "simulation, and analysis of permanent magnet motor drives, Part I: The permanent magnet synchronous motor drive," *IEEE Trans. on Ind. Appl.*, vol.25, pp. 265-273, 1989.
- [4] A. Consoli, G. Scarella, A. Testa, "Sensorless control of PM synchronous motors at zero speed", *Proc. IEEE IAS Annual Meeting, Phoenix*, Arizona, pp.1033-1040, Oct. 1999.
- [5] M. Corley, R.D. Lorenz, "Rotor position and velocity estimation for a permanent magnet synchronous machine at standstill and high speeds", *IEEE Trans. on Ind. Appl.*, vol. 34, no. 4, pp.784-789, Jul. 1998.